



POLITECNICO DI TORINO  
Repository ISTITUZIONALE

A new approach to Multi-hazard analysis

*Original*

A new approach to Multi-hazard analysis / Marasco, Sebastiano; ZAMANI NOORI, Ali; Kammouh, Omar; Cimellaro, GIAN PAOLO. - ELETTRONICO. - 1(2018). ((Intervento presentato al convegno 16th European Conference on Earthquake Engineering (16ECEE) tenutosi a Thessaloniki nel 18-21 June 2018.

*Availability:*

This version is available at: 11583/2724063 since: 2019-01-29T19:44:22Z

*Publisher:*

Curran Associates, Inc

*Published*

DOI:

*Terms of use:*

openAccess

This article is made available under terms and conditions as specified in the corresponding bibliographic description in the repository

*Publisher copyright*

(Article begins on next page)

## A NEW APPROACH TO MULTI-HAZARD ANALYSIS

Sebastiano MARASCO<sup>1</sup>, Ali ZAMANI NOORI<sup>2</sup>, Omar KAMMOUH<sup>3</sup>, Gian Paolo CIMELLARO<sup>4</sup>

### ABSTRACT

Multi-hazard engineering is increasingly recognized as a serious worldwide concern. In this paper, the principle of multi-hazard is applied to an essential steel structure (a hospital) located in California, US. The studied structure is assumed to be exposed to a sequence of three different cascading hazards (earthquake, blast, and fire). First, non-linear time-history analyses are performed and the seismic response of the structure is evaluated. The seismic input is assumed to cause damage to the hospital's power supply which it turns to generate an explosion. The probability of explosion is estimated accounting for the probabilities of fuel leakage, fuel concentration, and ignition. A set of twelve blast intensity levels is considered in the analysis, corresponding to the different quantity of fuel content inside the tank. Afterward, a fire hazard is generated following the explosion, whose intensity level is evaluated using the compartmental heat flux. The effect of the fire is translated into an increase in the steel's temperature, and damage is consequently evaluated. A methodology is proposed to accumulate the cascading damage caused by multi-hazard based on the conditional probability of occurrence. This method is capable of predicting the damage severity of the structural and non-structural components with a high accuracy. The proposed multi-hazard method is considered a significant step in improving the accuracy of loss estimation and in providing risk mitigation measures within the resilience-based environment. The results obtained in this paper verify the effectiveness and the practicality of the proposed method.

*Keywords: Multiple-hazard; Earthquake; Blast; Fire; Fragility curve; Resilience design*

### 1. INTRODUCTION

Large parts of the world are subjected to multiple natural, manmade, and artificial hazards. The rising of global population and the massive economic development in areas prone to disasters have increased the chance of multiple catastrophic incidents, which lead to disruption of buildings and infrastructures. Multi-hazard engineering and related mitigation risks play a key role in design and retrofitting of buildings. The multi-hazard assessment has to be performed by comparing risks of cascading mechanisms related to triggered hazard events. Padgett et al. (2010) evaluated hazard intensities to accurately predict the vulnerability of bridges using a multivariate regression analysis of the data obtained by surveys after hurricane Katrina. The American Institute of Steel Construction (AISC 2005) has provided seismic specifications of improved connection details for steel moment-frame and wood-frame shear. These specifications have been based on the numerical analyses of post-disaster data collected using surveys following 1989 Loma Prieta and 1994 Northridge earthquakes.

The risk assessments of structures that are exposed to more than one hazard are determined by

---

<sup>1</sup>PhD Student, Dept. of Civil Structural & Geotechnical Engineering, Politecnico di Torino, Torino, Italy, 10129 (email: sebastiano.marasco@polito.it)

<sup>2</sup>PhD Student, Dept. of Civil Structural & Geotechnical Engineering, Politecnico di Torino, Torino, Italy, 10129 (email: ali.zamani@polito.it)

<sup>3</sup>PhD Student, Dept. of Civil Structural & Geotechnical Engineering, Politecnico di Torino, Torino, Italy, 10129 (email: omar.kammouh@polito.it)

<sup>4</sup>Visiting Professor, Dept. of Civil and Environmental Engineering, University of California, Berkeley, CA, US, 94720

adopting the performance-based approach. For example, Barbato et al. (2013) suggested a novel assessment method that involved the evaluation of the individual impacts of the interaction among hurricane wind, flood, windborne debris, and rainfall hazards in the Performance-Based Hurricane Engineering (PBHE) framework. The performance of steel piers under seismic action was investigated by Bruneau et al. (2006). The simulation of large-magnitude earthquakes and the consequent explosions confirmed the capacity of the materials to resist to earthquakes and blast separately, but not a simultaneous combination of the two hazards.

Multi-hazard design starts with the structural and non-structural analysis for individual hazard. The location, magnitude and frequency of occurrence of each hazard have to be estimated through a probabilistic approach. Several probabilistic approaches have been proposed for multiple-hazard risk assessment. In this paper, the methodology developed by Marasco et al. (2017) is adopted to estimate the total amount of structural damage caused by sequential hazard. Earthquake, blast and fire have been considered as sequential hazards and numerical analyses have been performed. The combination of the structural damage for sequential hazards is evaluated according to Bayes' theorem. The methodology has been applied to a steel structure hospital located in California, US. The first section of the paper provides a detailed description of the methodology, while the second part illustrates its applicability through a case study building. Lastly, a numerical example of cumulative structural damage estimation is performed.

**2. METHODOLOGY**

In the Performance-Based framework the structural vulnerability is conventionally expressed in terms of probability to exceed a stated performance objective when the structure is subjected to a certain level of hazard. In case of sequential hazardous events, the probabilistic correlation between the main hazard and the occurrence of the other hazards has to be estimated to assess the performance of the structural system. In this paper, the occurrence of a sequential hazard for a given Intensity Measure (IM) of the main hazard is estimated following a probabilistic Bayesian approach. The Figure 1 depicts a simplified scheme of the hazard analysis conducted in a multiple-hazard scenario.

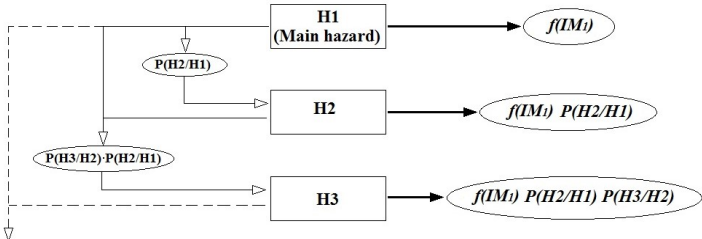


Figure 1. Hazard analysis framework for sequential multiple-hazards

The estimation of the conditional probability  $P(H_i/H_j)$  that one hazardous event ( $I$ ) occurs as consequence of another hazard ( $J$ ), is provided by using specific physical models. As example, a steel tank containing flammable materials in a seismic zone is considered. The probability to have the explosion of the tank due to an earthquake with a given intensity is strictly dependent firstly on the mechanism of ignition of the material inside the tank; and secondly the failure modes and equipment damage of the tank.

A physical model has to be capable to describe the fragility of the tank with reference to the possible trigger of the hazardous mechanism. Identifying the most probable failure mode and modeling the geometry of the tank, a numerical analysis has to be performed to evaluate the blast fragility of the tank. In order to take into account different earthquake scenarios, several numerical analyses have to be carried out. According to the mechanism of ignition, a maximum threshold of the earthquake response parameter of the tank has to be fixed. When this maximum limit is exceeded, the probability

to have explosion is equal to 1, and 0 otherwise. The probability to have explosion after earthquake is obtained by lognormal fitting of the results. This simple procedure is able to provide a conditional probability of explosion due to earthquake for different seismic intensity.

The vulnerability of a structural system to a hazard is expressed in terms of fragility functions derived from numerical analyses for a given damage state. In a multi-hazard scenario, the prediction of the level of structural damage has to take into account the chain effects. They represent the modification of the structural characteristics caused by the previous hazard. Therefore, the sequential hazards are treated as depend phenomena. The cumulative damage probability due to sequential hazardous events ( $P(DS < ds)$ ) is expressed as product between conditioned probability of the sequential events and the exceedance damage probability for single hazard. Equation 1 gives the cumulative probability to exceed a specified level of damage according to the proposed methodology.

$$\begin{aligned}
 P(DS > ds) = & P(DSH1 > dsh1 | SP_0) + \\
 & + P(DSH2 > dsh2 | SP_1) \cdot P(H2 | H1) + \\
 & + P(DSH3 > dsh3 | SP_2) \cdot P(H3 | H2) \cdot P(H2 | H1) + \\
 & + \dots
 \end{aligned}
 \tag{1}$$

where  $H_1$ ,  $H_2$  and  $H_3$  represent three sequential hazards while  $P(DSH_1 < dsh_1 | SP_0)$ ,  $P(DSH_2 < dsh_2 | SP_1)$  and  $P(DSH_3 < dsh_3 | SP_2)$  are the exceedance probability of damage for the considered hazards. The variability in the structural parameters is expressed by the structural system parameters  $SP_0$ ,  $SP_1$  and  $SP_2$  that consider the chain effects.

### 3. CASE STUDY

A five-story steel hospital building with dimension in plan of 82.3 m by 33.7 m, spans length of 9.1 m and 12.3 m, and the story height equal to 4.6 m is considered. The building has two external lateral moment resisting frames in the longest direction and bracing system in the other direction. The H sections (wide channel, W) have been used for beams and columns while hollow structural sections (HSS) have been designed for bracing system (Figure 2). The building is located in Oakland, California, US (Lat: 37.7792, Long: -122.1620). An additional source of electricity is provided, just in case of an unexpected power outage. It includes an aboveground LPG tank equipped of power sources, controls, transfer equipment, supervisory equipment and accessory situated outside the building. The tank has the capacity to generate 2500 kVA of electricity for 8 hours. The LPG tank has a total capacity of 3597 litres and it is located 9.2 m far from the building.

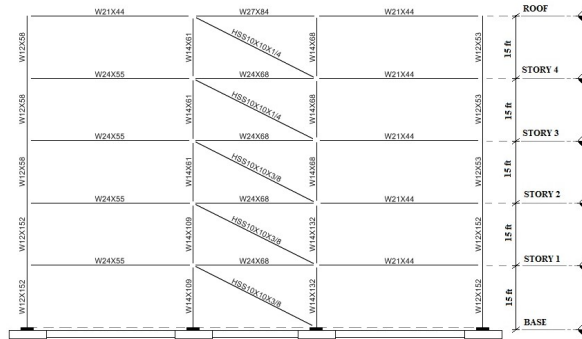


Figure 2. Internal bracing frame configuration in Y-direction

Earthquake (main hazard), blast and fire have been assumed as sequential hazards. The sequence of hazards caused by the earthquake is not specified and depends on the localization of the high risk potential elements inside and outside the structure as well as their fragility. Logical tree of multi-

hazard sequence for general healthcare facilities is represented in Figure 3.

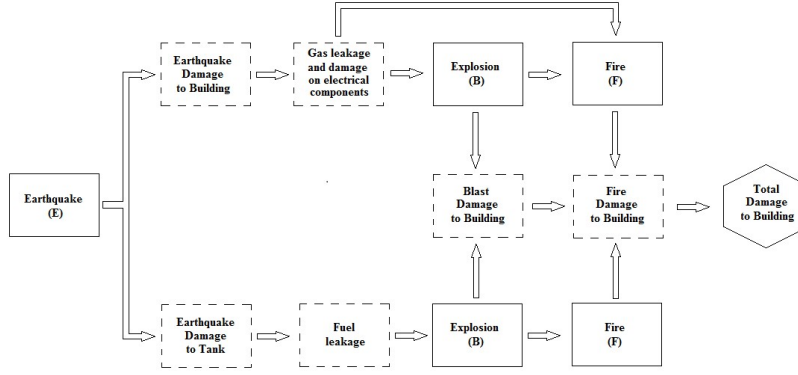


Figure 3. Hazard sequence: earthquake-blast-fire

The external fuel tank and building elements are both damaged by the earthquake. The fuel leakage can cause an ignition resulting a deflagration of the fuel inside the tank. This series of events may cause explosion of the tank and generate an impulsive air pressure load on the front face of the building. The heat of the gas explosion may also ignite any inflammable materials located within the buildings. In a short time the ignition generates flashover and fire propagates through the building compartment. Fragility curves for each hazard have been derived considering earthquake ( $P(DE > de)$ ), blast ( $P(DB > db)$ ), and fire ( $P(DF > df)$ ) hazard. For this case study, the cumulative probability to exceed a specified level of damage is expressed in Equation 2.

$$P(DS > ds) = P(DE > de) + P(DB > db) \cdot P(B | E) + P(DF > df) \cdot P(F | B) \cdot P(B | E) \quad (2)$$

Post-earthquake effects on the small size tanks have shown a low fragility of these elements. Thus, the associated probability to have an explosion and the associated damage exceedance probability is strongly reduced. For this reason, the proposed methodology has been applied neglecting the chain effects.

### 3.1 Hazard Analysis

#### 3.1.1 Earthquake

Five different Hazard Levels (HL) have been identified (50%, 20%, 10%, 5%, and 2% of exceedance probability in 100 years) and analyses for each of the levels have been conducted. The mean value of moment magnitude ( $M_{W,mean}$ ) and epicenter distance ( $R_{mean}$ ) with the logarithmic spectral offset at reference period ( $\varepsilon(T_{ref})$ ) have been evaluated according to Boore-Atkinson attenuation law for each HL (Boore and Atkinson 2008). All the data can be found through the interactive de-aggregation of USGS (2013). The shear wave velocity at the uppermost 30 m has been assumed equal to 736 m/s according to Global Vs30 Map Server.

A new Ground Motion Selection and Modification (GMSM) procedure has been used to minimize the dispersion values of the Engineering Demand Parameter (EDP) calculated through dynamic analyses. Its functionality is based on the energy content of the motions in the frequency domain. Seven groups of acceleration histories (for both horizontal directions) have been selected for each HL in such a way to match the target spectrum at reference period of the building. The Conditional Mean Spectrum (Baker 2010) obtained from de-aggregation study (CMS- $\varepsilon$ ) has been considered as target spectrum. Boore-Atkinson attenuation model has been used to define the predicted spectral accelerations at the site, while the Baker and Jayaram model has been considered as correlation law (Baker and Jayaram 2008). The first period of the structure has been selected as conditioning period ( $T_{ref}$ ). The five target spectra and the associated spectrum-compatible groups of ground motions have been obtained through

the software OPENSIGNAL 4.1 (Cimellaro and Marasco 2015). Parts of the results in terms of mean spectrum-compatibility have been illustrated in Figure 4. Moreover, the spectral acceleration at reference period has been considered as Intensity Measure (IM).

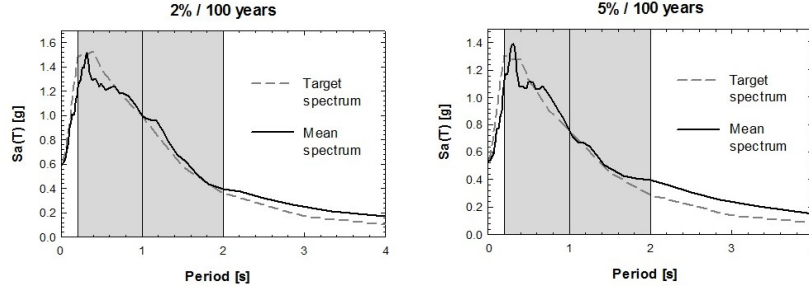


Figure 4. Mean spectrum compatibility for the five HLs

### 3.1.2 Blast

After earthquake, the power supplier system (fuel tank, electrical components, etc.) may be slightly or severely damaged. A fuel leakage may be as a result of damaged valves, connections or pipes of a fuel tank. However, an explosion cannot occur when there is not ignition source and when the fuel concentration is less the flammable concentration range. Thus, explosion are usually determined by concentration of fuel, gas leakage and ignition source. Considering the three parameters as stochastic variables, the probability of explosion after earthquake ( $P(B/E)$ ) of a damaged fuel tank is reported in Equation 3.

$$P(B|E) = P_L \cdot P_{FC} \cdot P_I \quad (3)$$

where  $P_L$  represents the probability of fuel leakage,  $P_{FC}$  is the probability to have maximum fuel concentration and  $P_I$  defines the probability of ignition. In this case study, it has been assumed that the damage takes place on the pipe that is connected to the tank. This assumption is based on the fact that the tank has a small size. According to ATC P-58 (2012) the probability to have large gas leakage for small diameter piping system ( $D < 10$  cm) is given in terms of fragility function with accelerations as EDP ( $\mu = 1.1g$ ,  $\beta = 0.5$ ). The probability to have maximum gas concentration has been estimated considering the failure of the pipe closeness to the joint connection. A simplified dynamic model has been developed to predict the maximum horizontal drift of the pipe. The tank has been considered as rigid body, while its legs have been assumed having shear flexibility in horizontal direction. The anchor bolts have been designed according to UBC-97 (1997) in order to ensure full restraint at the base. The first period of the tank ( $T_{tank}$ ) has been calculated considering different fuel quantity as HL (5%, 10%, 20%, 30%, 40%, 50%, 60%, 70%, 80%, 90%, 95%, and 100%). The occurrence of shear failure in the vertical pipe causes the maximum gas concentration. Based on this postulation and considering the maximum shear stress value on the cross section of the pipe, the failure spectral acceleration has been calculated (Equation 4).

$$S_{a, failure} = \frac{45.44}{g} \cdot \left( \frac{f_{u,d}}{E} \right) \cdot \left[ \frac{L_v^3}{(D_e^2 - D_i^2)(D_e^2 + D_e \cdot D_i + D_i^2)} \right] \cdot \frac{1}{T_{tank}^2} \quad (4)$$

where  $f_{u,d}$  and  $E$  represent the ultimate stress and elastic modulus of the steel, respectively,  $D_e$  and  $D_i$  are the external and internal pipe diameter, and  $L_v$  is the length of the vertical pipe. The occurrence of maximum gas concentration is recorded when the spectral acceleration of the selected ground motion exceeds the  $S_{a, failure}$ . In these cases, the probability to have maximum gas concentration has been assumed equal to 1 and 0 otherwise. Then, a tridimensional fragility curve has been developed by fitting a lognormal distribution of the data for each value of fuel quantity ( $IM_1$ ) and spectral acceleration at period of the tank ( $IM_2$ ). The ignition probability is provided with reference to the

maximum fuel quantity. The information required for risk data assessment is provided by the International Association of Oil and Gas producers (IAOGP 2010) in order to evaluate the probabilities of hydrocarbon releases igniting. In this case study, only delayed ignition probability has been considered, since immediate ignition needs sources close to the fuel leakage point. Release of flammable gases from small onshore LPG plant has been assumed as ignition scenario and the related probability function has been derived. The Bernoulli's principle is used for the computation of maximum gas concentration ( $FC_{max}=29.70 \text{ kg/s}$ ). Figure 5a illustrates the probability to have explosion after earthquake.

### 3.1.3 Fire

The probability to have fire inside the building is related to the heat transmission due to the tank explosion. The Stefan Boltzmann's law has been used to compute the heat flux for each point of the building in front of the tank. The twelve different tank fuel quantities have been assumed as first IM ( $IM_i$ ). The temperature at which LPG burns has been assumed to be  $2300 \text{ K}^\circ$ , while the atmospheric transmissivity coefficient has been fixed to 0.66. The transfer configuration factor has been calculated for the entire external panel of the building (meshed with  $0.5 \times 0.5 \text{ m}$  elements). The computation of the heat flux on building façade has been accomplished with the help of a Matlab code. Supposing the external panel as fireproof, only the opening surfaces (windows, doors, etc.) have been considered as susceptible to trigger fire inside the building. The minimum value of heat flux that can cause flammable materials in a room to burst into flames has been assumed equal to  $30 \text{ MJ/m}^2$ .

Comparing the façade of the building with the heat flux map, the starting fire surface has been deduced for each fuel quantity value. The estimated conditional probability to have ignition of elements inside the building has been fixed to 1 whether the maximum heat flux on the opening is greater than the considered limit, and 0 otherwise. Thus, the probability to have ignition of inflammable materials inside the building after blasting ( $P(F/B)$ ) has been estimated through a lognormal distribution fitting (Figure 5b). The gypsum plasterboard with steel studs have been considered as internal partition between adjacent columns. Since the gypsum panels are used as insulation system, they can be considered as fireproof materials. Thus, each volume identified by two adjacent columns has been considered as fire compartment.

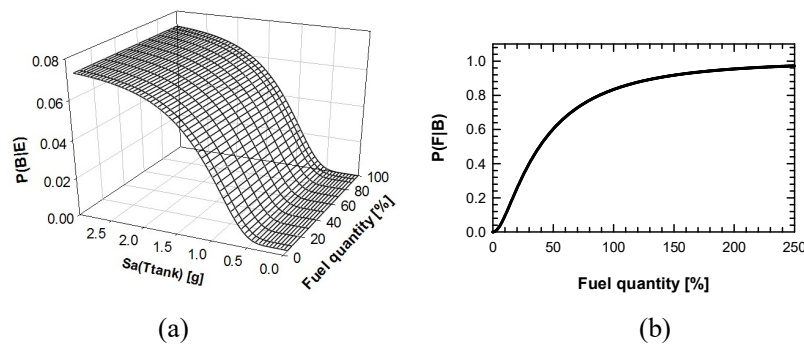


Figure 5. (a) probability to have an explosion after the earthquake, (b) probability to have the fire after the blast

## 3.2 Methods and models

### 3.2.1 Earthquake

The time history analyses have been performed on an appropriately modeled three-dimensional structure utilizing SAP2000. The lateral resisting system is a dual system. It is made up of moment resisting frames and braces, in both directions. The beams and columns have H sections, while hollowed structural section (HSS) have been assigned to the braces. The concentrated plasticity model has been used to take into consideration the nonlinearity of the structural elements. According to

FEMA-356 (2000), Steel-beams Flexural Hinge (type Moment M3) and Steel-column Flexural Hinge (type P-M2-M3 with  $M-\chi$  cylindrical domain) has been used for beam and column elements, respectively. The plastic hinges for brace elements have been modeled as Steel-braces Axial Hinges. A 3% damping ratio has been assigned to the frames according to Rayleigh formulation. The nonlinear dynamic analyses have been performed using non-linear direct integration method, taking into account P- $\Delta$  effects and applying the horizontal acceleration time histories in the two principal directions of the building.

### 3.2.2 Blast

The methodology provided by Marasco et al. (2017) is adopted to perform the blast analysis. To do that, U.S. Army Technical Manual (TM5-1300 1990) has been used in this study to establish the blast load parameters required in structural analysis. Twelve different fuel quantities reported in Table 1 representative of different IMs have been considered and the equivalent weight of TNT has been estimated accordingly. To perform nonlinear time history analysis, the typical blast overpressure time history provided by TM5-1300 has been applied. The blast time history overpressure has been idealized by rise of an equivalent triangular pulse of maximum reflected pressure ( $P_r$ ) at an arrival time ( $t_A$ ) after the explosion (Figure 6). A fictitious duration ( $t_{rf}$ ) has been determined in place of the actual positive duration ( $t_o$ ) assuming the linear decay of overpressure given by Equation (5):

$$t_{rf} = 2i_r / p_r \quad (5)$$

where  $i_r$  is the reflected impulse and  $P_r$  is the maximum reflected pressure determined through the charts provided by TM5-1300. A similar procedure for the negative phase has been used whereas rise time of negative peak pressure has been considered equals to 0.25 to negative fictitious duration ( $t_{rf}$ ). The different blast pressure time histories specific to each structural member have been established corresponding to the different scaled distance parameter ( $Z$ ) and potential charge weight for each blast IM.

The blast dynamic pressure has been applied to the beams, columns and exterior walls of the exposed structural area on the front face of the explosion. The exterior walls have been considered as typical concrete masonry wall reinforced with vertical bars. Each wall has been simplified to an equivalent SDOF system in such a way that the deflection of the concentrated mass to be same as the mid-span of the actual wall. An elasto-perfectly plastic behavior for each wall has been defined and the dynamic characteristics have been adjusted for the condition of high-velocity impacts. A MATLAB code has been used to calculate the dynamic responses of the mid-span of the wall considering the plastic hinge formation (yielding rotation capacity). Then, resulted time history reactions have been directly applied to the adjacent beams in SAP2000 models. Blast pressure time histories relevant to the beams and columns have been applied directly on the framing elements. In order to take into account the effects of high-rapid load environment, mechanical properties of steel materials have been enhanced by means of dynamic increased factor (DIF). Finally, twelve different nonlinear time history analyses have been conducted. In the cases of the loss of the load-bearing capacity of key structural elements, the progressive collapse analyses have been carried out and thus the dynamic effects of removal of the failed elements have been evaluated using time history analyses.

Table 1. Different fuel quantities as HL for the blast analysis.

<b>Hazard</b>	<b>1<sup>st</sup></b>	<b>2<sup>nd</sup></b>	<b>3<sup>rd</sup></b>	<b>4<sup>th</sup></b>	<b>5<sup>th</sup></b>	<b>6<sup>th</sup></b>	<b>7<sup>th</sup></b>	<b>8<sup>th</sup></b>	<b>9<sup>th</sup></b>	<b>10<sup>th</sup></b>	<b>11<sup>th</sup></b>	<b>12<sup>th</sup></b>
Fuel	5	10	20	30	40	50	60	70	80	90	95	100



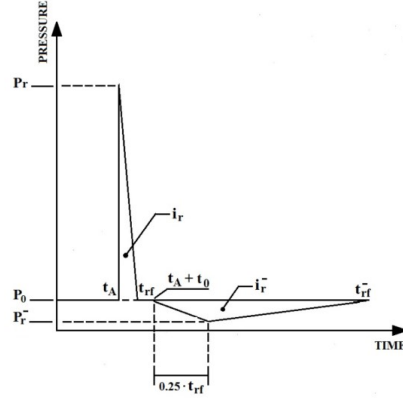


Figure 6. Idealized blast overpressure time history

### 3.2.3 Fire

The ignition of inflammable materials within the compartment generates a flashover that will then cause a rise in temperature. The fire curve for the compartment is majorly used to determine the design-basis fire action. The fire curve is simply the evaluation of post-flashover time-temperature relationship and is determined by the quantity of combustible materials (total calorific value), the velocity of combustion, and the ventilation conditions. The quantity of combustible materials (total calorific value) and the velocity of combustion are main determinant of the entire heat flux that is produced inside the compartment ( $q_f$ ). It is assumed that the compartment heat flux is normally distributed. The mean value and standard deviation are used to specify the exact fire load for different building category in accordance to EC1 (2002). The normal mean specific fire load and standard deviation for hospitals are 230 MJ/m<sup>2</sup> and 69 respectively. In the study case, the specific heat flux of the compartment has been selected as IM<sub>2</sub> and eight different exceedance probabilities have been considered (Table 2).

Table 2. Different fuel quantities as HL for the blast analysis.

	90%	85%	80%	50%	20%	10%	5%	2%
$q_f$ [MJ/m <sup>2</sup> ]	135	160	180	230	281	322	360	400

The temperature-time relationship developed by Lie (1974) has been considered. The peak temperature ( $T_{peak}$ ) and peak time ( $t_{peak}$ ) are both used to describe the top of the curve. The definition of these parameters has been done in accordance to the time equivalence concept, which is related to the actual fire exposure to the standard test fire (standard curve). The ventilation factor  $w$ , is one of the main parameters used to evaluate the equivalent time. In the study case, two vertical openings having dimension of 1.50m×2.00m and opening factor of 0.07 have been considered. Table 3 resumes the major parameters of the temperature-time curves for each generated heat flux. An evaluation of the degradation of the physical and mechanical characteristics of the materials by fire has been conducted. In accordance to Fourier's equation, the net transmitted heat flux ( $q_{f,n}$ ) is used to determine the thermal distribution for any fire scenario. In a system where the entire structural element is homogenous and isotropic, the Fourier's equation can be incorporated into the element's volume and then rephrase discretely to obtain Equation 6.

$$\Delta T_{(i)} = k_{sh} \cdot \frac{A_m / V}{\rho \cdot c} \cdot q_{f,n(i)} \cdot \Delta t \quad (6)$$

where  $\Delta T_{(i)}$  is a definition of  $i^{th}$  increment of uniform temperature in the cross section area of the element while  $A_m/V$  is the section factor given by the ratio between the area of the element exposed to

fire ( $A_m$ ) and its total volume ( $V$ ). Density ( $\rho$ ) and specific heat ( $c$ ) refer to the materials that made up the structural element while  $\Delta t$  is the time it takes the change in temperature to take place ( $\Delta t < 5s$ ). The coefficient  $k_{sh}$  is used to consider of the “shadow effects” that cause non-uniform thermal transversal distribution. In order to achieve a pseudo-uniform transversal temperature distribution,  $k_{sh}$  coefficient has been assessed as the actual fire exposure.

The element’s section factor that is taken as bin section ratio is represented as  $(A_m/V)_b$ , while  $(A_m/V)$  represents the column’s actual section factor. The fire exposure for the column has been supposed for one side of the web and for both flanges. Three different sections of beams and columns have been identified for the compartment. Fire resistance of steel elements inside the compartment has been assessed considering the maximum uniform thermal loads for each heat flux value. The analyses have been accomplished with the help of the software SAP2000. The mechanical and physical materials properties have been modified according to AISC (2005) depending on the temperature values. The nonlinearity of the structural elements has been taken into account according to concentrated plasticity model. Progressive nonlinear analyses have been performed. The nonlinearity effects have been taken into account in accordance to concentrated plasticity model. Progressive nonlinear analyses have also been carried out.

Table 3. Characteristic time-temperature curve parameters for each generated heat flux.

	90%	85%	80%	50%	20%	10%	5%	2%
$t_e$ [min]	23.50	25.00	26.19	33.46	40.83	46.85	52.2	58.2
$T_{peak}$ [K°]	1111	1131	1145	1173	1188	1205	1218	1228
$t_{peak}$ [min]	11.5	13.5	16	20.5	24.5	29.5	33.5	37

### 3.3 Structural Responses

#### 3.3.1 Earthquake

Maximum transient inter-story drifts have been considered as EDP to assess the performance of the structure under the seismic load. Fragility curves, for both principal horizontal directions, have been investigated for the different damage states (slight, moderate, extensive, and complete) according to ATC P-58 (2012) (Figure 7).

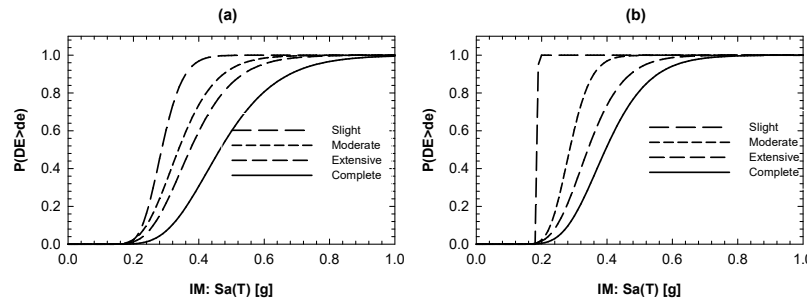


Figure 7. Fragility curves in X direction (a) and Y direction (b) for earthquake hazard

#### 3.3.2 Blast

An accurate assessment of the global response of building under blast load has been accomplished by assuming the loss of horizontal stiffness as EDP. In the Y direction, response of the structure is integrated into the SDOF dynamic response based on the specification of Equation 7.

$$K_{eq} = \frac{\delta_{eq}}{V_{eq}} = \frac{\delta_{top} \cdot \sum_{i=1}^{N=5} (\phi_i - \phi_{i-1})^2}{V_b \cdot \sum_{i=1}^{N=5} \phi_i} \quad (7)$$

where  $d_{top}$  represents the maximum top floor displacement and  $V_b$  is the base shear obtained at the same time of the maximum displacement. In this case, the actual distribution of floor displacements has been taken into consideration and this usually occur through the shape coefficients  $\phi_i$ , where  $i^{th}$  is associated to the floor displacement normalized with respect the top one. The yielding drift for braced system has been calculated according to ATC P-58 (2012) and the maximum drift threshold have been assumed (Table 4) for four different damage states. The stiffness reduction limits have also been computed. The computation involves an assumption of an elasto-perfectly plastic global behaviour of the steel frame. Figure 8a depicts the fragility curves for each DS.

Table 4. Characteristic time-temperature curve parameters for each generated heat flux.

Damage State	Slight	Moderate	Extensive	Complete
Inter-story drift [%]	1.00	1.80	2.80	4.80
Stiffness reduction [%]	30.00	61.00	75.00	85.00

### 3.3.3 Fire

The assessment of structural capacity has been carried out evaluating the highest obtainable deflection for beams and columns as EDP. In this case, two different damage states indicating the level of irreversible damage on the beam (DS1) and on the column (DS2) have been considered. The first damage state provides useful data on the highest flexural capacity of the beam. It is assumed that the threshold vertical deflection ( $v_b$ ) for this damage state is equivalent to deflection attributed to uncontrolled vertical displacement. The second damage state is linked to the highest drift of the column ( $\delta_c$ ) which occurs under multiple stresses as a result of compression and bending moment and with full consideration of the P- $\Delta$  effects. It has been assumed that the drift's highest limit coincides with the horizontal displacement that generates uncontrollable unstable displacement. For each analysis, the probability to have irreversible damage to the structural elements has been assumed equal to 1 if the response parameter is greater than the associated limit and 0 otherwise. Fragility curves have been developed fitting lognormal distribution to the data (Figure 8b).

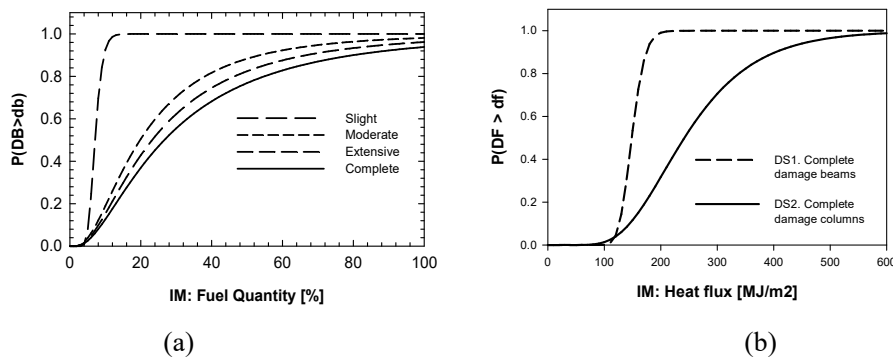


Figure 8. (a) fragility curves for blast hazard, (b) fragility curves for fire hazard

## 4. NUMERICAL EXAMPLE

Equation 2 is used to derive the cumulative fragility function for each specific damage state. Figure 9 is a graphical illustration for the fragility curves for earthquake (a), blast due to earthquake (b) and fire due to blast (c), with reference to a complete damage to the columns.

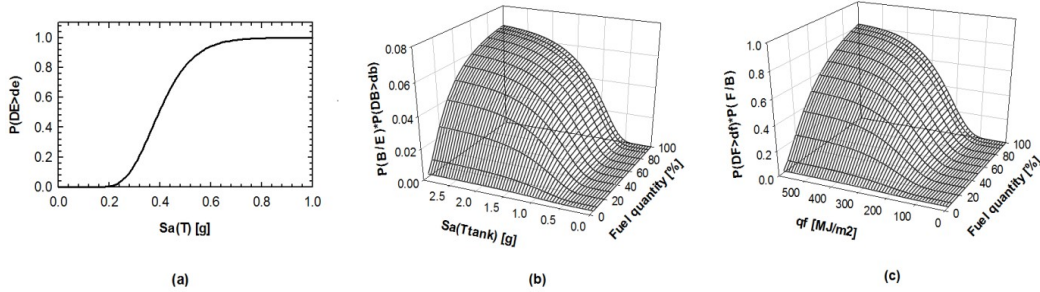


Figure 9. (a) fragility curve for earthquake, (b) blast due to earthquake and (c) fire due to blast.

The factors that are assumed to be IM parameters include; heat flux generated in the compartment, spectral acceleration at period of the structure, spectral acceleration at period of the tank and fuel quantity inside the tank. The three values also enable evaluation of the cumulative probability to exceed a particular level of damage. A numerical example of cumulative probability damage estimation has been performed considering the five different HL for earthquake, full capacity of tank and heat flux equal to the average value. In this case study building, the probability of cumulative damage values is shown in Table 5.

Table 5. Numerical example for cumulative damage calculation due to earthquake, blast and fire.

HL <sub>E</sub>	S <sub>a</sub> (T) [g]	S <sub>a</sub> (T <sub>tank</sub> ) [g]	P(DE>de)	P(DB>db)·P(B E)	P(DF>df)·P(F B) P(B E)	P(DS>ds)
2%	1	0.95	0.99	0.0255	0.0079	1.00
5%	0.75	0.85	0.96	0.0163	0.0059	0.98
10%	0.55	0.75	0.89	0.0104	0.0040	0.90
20%	0.40	0.65	0.50	0.0055	0.0023	0.51
50%	0.20	0.40	0.01	0.0002	0.0001	0.01

The probability encountering blast after an earthquake is strictly correlated to the tank's size. In this case, the value of maximum gas concentration tends to lower the probability of explosion. Consequently, the conditioned probability to have fire after explosion is strongly reduced.

## 5. CONCLUSION

A new methodology to estimate cumulative structural damage due to sequential hazardous events is proposed. Hazards interaction is assessed by using the various calibrated physical models to reduce the epistemic uncertainties of the model. Each hazard is considered as an independent phenomenon and the variation of the mechanical and physical parameters of the structural model under sequential hazards is estimated. The numerical example showed that the probability to exceed a given damage state due to an explosion and consequent fire are much smaller than the exceedance damage state probability for earthquake (less than 3%). This is due to the low probability to have explosion of the tank after earthquake. For the proposed case study, assuming the three hazards as independent phenomena is a reasonable hypothesis, since the chain effects do not influence the total damage estimation. The application of the proposed multi-hazard approach can be used for both improving the structural safety and reducing the building life cycle costs to enhance the resilience of the structure.

## 6. ACKNOWLEDGEMENTS

The research leading to these results has received funding from the European Research Council under the Grant Agreement n° ERC\_IDEAL RESCUE\_637842 of the project IDEAL RESCUE-Integrated Design and Control of Sustainable Communities during Emergencies.

## 7. REFEENCES

- AISC (2005), Specification for Structural Steel Buildings, AISC 360, American Institute of Steel Construction, Chicago, IL.
- ATC (2012), Seismic Performance Assessment of Buildings, ATC-58, Applied Technology Council, Redwood City, CA.
- Baker JW (2010), Conditional mean spectrum: Tool for ground-motion selection, *Journal of Structural Engineering*, 137(3), 322-331.
- Baker JW, Jayaram N (2008), Correlation of spectral acceleration values from NGA ground motion models, *Earthquake Spectra*, 24(1), 299-317.
- Barbato M, Petrini F, Unnikrishnan VU, Ciampoli M (2013), Performance-Based Hurricane Engineering (PBHE) framework, *Structural Safety*, 45, 24-35.
- Boore DM, Atkinson GM (2008), Ground-motion prediction equations for the average horizontal component of PGA, PGV, and 5%-damped PSA at spectral periods between 0.01 s and 10.0 s., *Earthquake Spectra*, 24(1), 99-138.
- Bruneau M, Lopez-Garcia D, Fujikura S (2006), Multihazard-resistant highway bridge bent, *Proc., Structures Congress*, ASCE New York, 1-4.
- Cimellaro GP, Marasco S (2015), A computer-based environment for processing and selection of seismic ground motion records: Opensignal, *Frontiers in Built Environment*, 1, 17.
- EC1 (2002), Eurocode 1: Actions on structures, Part 1-1: General actions - Densities, self-weight, imposed loads for buildings, EC1, European Committee for Standardization, Bruxelles, BG.
- FEMA (2000), Prestandard and Commentary for the Seismic Rehabilitation of Buildings, FEMA 356, Federal Emergency Management Agency, Washington, D.C.
- IAOGP (2010), Ignition probabilities, Risk Assessment Data Directory, International Association of Oil & Gas Producers, Report No. 434-6.1.
- Lie TT (1974), Characteristic temperature curves for various fire severities, *Fire Technology*, 4pp., 315-326.
- Marasco S, Zamani Noori A, Cimellaro GP (2017), Cascading Hazard Analysis of a Hospital Building, *Journal of Structural Engineering*, 143(9), p.04017100
- Padgett J, Ghosh J, Ataei N (2010), Sensitivity of dynamic response of bridges under multiple hazards to aging parameters, *Proc., 19th analysis and computation specialty conference. ASCE*.
- TM5-1300 (1990), The Design of Structures to Resist the Effects of Accidental Explosions, US Department of the Army, Navy, and Air Force, Washington DC.
- UBC-97 (1997), In Structural engineering design provisions, International conference of building officials, Whittier, California.
- USGS (2013), Seismic Hazard Analysis tools. U.S. Geological Survey, <<http://earthquake.usgs.gov/hazards/designmaps/grdmotion.php>>.